Microwave scattering by turbulent plasma

1968 J. Phys. A: Gen. Phys. 2 75

(http://iopscience.iop.org/0022-3689/2/1/011)

J. PHYS. A (GEN. PHYS.), 1969, SER. 2, VOL. 2. PRINTED IN GREAT BRITAIN

Microwave scattering by turbulent plasma

P. E. STOTT

United Kingdom Atomic Energy Authority Research Group, Culham Laboratory, Abingdon, Berks.

MS. received 21*st August* 1968

Abstract. Microwave transmission across a column of turbulent plasma is strongly influenced by the presence of small-scale plasma density inhomogeneities. In devices such as ZETA, fluctuations of 10–25% about mean densities of 10^{14} cm^{-3} have been observed with correlation lengths of up to 5–10 cm and time scales of 10^{-5} s. Scattering measurements have used microwaves with a free-space wavelength of 2 mm (corresponding to a critical density of $2{\cdot}5 \times 10^{14}$ cm^{-3}) and in ZETA multiple scattering processes are important. A numerical solution for the transport theory formulation of multiple scattering is used to interpret the measurements and good agreement with Langmuir probes is obtained.

1. Introduction

Microwave measurements at millimetre wavelengths in ZETA (Wort 1965) have demonstrated that the transmission across the plasma column is strongly influenced when the discharge is turbulent. The transmission, which is attenuated by as much as 20–30 dB below the level which would be expected if the discharge were quiescent, reveals amplitude and phase fluctuations at frequencies of up to several megahertz. At the same time microwaves scattered through 90° to the direction of transmission are observed. These effects persist whilst current is flowing in the plasma. When the discharge current falls to zero, the scattering and attenuation disappear and interferometric fringes are seen in the decaying afterglow plasma.

Langmuir probe measurements confirm that the discharge is turbulent and reveal plasma density fluctuations extending over correlation lengths of up to 5–10 cm, with time scales of some 10^{-5} s (Robinson and Rusbridge 1965). These fluctuations in plasma density produce corresponding variations of refractive index which scatter the microwaves, resulting in an attenuation of the transmitted beam. When the plasma density is close to the critical density (i.e. the density at which the plasma frequency equals the microwave frequency and transmission is cut-off) the scattering is strong and multiple processes are important. This situation is interesting both as a study of multiple scattering and as a sensitive non-perturbing diagnostic technique for investigating the turbulent state of a plasma.

Scattering measurements have been carried out on ZETA at mean plasma densities of $1{\cdot}0 \times 10^{14}$ cm^{-3} using microwaves at a frequency of 137 GHz (approximate free-space wavelength 2 mm) corresponding to a critical density of $2{\cdot}5 \times 10^{14}$ cm^{-3}. The scattered microwave intensity, which is typically of the order of 0·1% compared with the direct transmission when the plasma is quiescent, may be fitted by a Gaussian profile with angular widths in the range 10°–30°. Similar measurements have been carried out on TPOT (Turbulent Plasma Observation Tube), a straight quartz discharge tube which was constructed to supplement the range of microwave experiments possible on the metal-walled toroidal ZETA. In this case as much as 50% of the microwave beam passed through the plasma without being scattered. The difference between the two sets of results is mainly due to the fact that the diameter of ZETA is large compared with the mean free path between successive scatterings and thus multiple events dominate; whilst in TPOT, which is smaller, only single-order scatterings are important.

The interpretation of microwave scattering measurements in a turbulent plasma at near critical density is a familiar problem (Wort 1966, Larionov *et al.* 1968). A transport theory for the propagation of electromagnetic waves in a turbulent plasma has been developed by Stott (1968) and will be used to evaluate the experimental results. This approach conveniently splits the calculation into two separate and almost independent stages. First the cross section for a single-scattering event occurring in a unit volume of plasma is calculated in terms of a suitable model of the turbulence. The transport equation containing this cross section is then solved numerically using a Monte Carlo method.

2. The scattering cross section of a turbulent plasma

The density fluctuations recorded by Langmuir probes are slowly varying on the time scale of the microwaves (i.e. typical frequencies of 1 MHz compared with 137 GHz) and will be regarded simply as different realizations of an effectively quasi-static system with random spatial fluctuations, i.e.

$$n(\boldsymbol{r}, t) = n(\boldsymbol{r}).$$

To justify this assumption the scattered microwave intensity must be averaged over a time which is much longer than the time scale of the density fluctuations, yet short compared with the lifetime of the plasma, i.e.

$$10^{-6} \ll T_{\mathrm{av}} \ll 10^{-3}\,\mathrm{s}.$$

The magnetic field in ZETA is sufficiently small (800 G) for us to ignore its effect on the dielectric constant whilst the plasma temperature is high enough (10–50 eV) to neglect collisional absorption at microwave frequencies. The dielectric constant is given by

$$\xi = 1 - \frac{n(\boldsymbol{r})}{n_{\mathrm{c}}}$$

where $n_{\mathrm{c}} = m_{\mathrm{e}}\omega^2/4\pi e^2$ is the critical density which is dependent on the microwave frequency ω and equals $2{\cdot}5 \times 10^{14}\,\mathrm{cm}^{-3}$ at 137 GHz. Density fluctuations of 10–25% relative to the mean density (typically $1{\cdot}0 \times 10^{14}\,\mathrm{cm}^{-3}$) with correlation lengths extending to 5–10 cm in a direction normal to the magnetic field have been measured with probes in ZETA. Fluctuations rather larger in both relative magnitude and scale length have been observed in TPOT. In both cases the fluctuations appear to be elongated along the direction of the magnetic field which is helically twisted as a result of the combination of the externally applied axial field with the self-constricting azimuthal field due to the discharge current. The helicity is characterized by the parameter $\Theta = 2I_{\mathrm{g}}/R_0B_z$ where I_{g} is the plasma current, R_0 the diameter of the plasma and B_z the axial magnetic field. The helicity is small in TPOT (typically $\Theta = 0{\cdot}2$) and the turbulence may be regarded as approximately two dimensional with scattering confined to the plane normal to the axial field. In ZETA the helicity is much larger (typically $\Theta = 1{\cdot}7$) and must be taken into account in solving the transport equation.

When the density fluctuations are small compared with the critical density and the scale length is comparable with the wavelength, the scattering cross section is given by the Fourier transform of the density correlation function. In the ZETA and TPOT plasmas, however, with densities close to the critical value and scale length much longer than one wavelength, this simple solution is no longer valid and the evaluation of the cross section in terms of the correlation function presents a problem of some complexity (Stott 1968). Diffraction effects are unimportant if the refractive index varies slowly over a wavelength and it would be expected that the scattering will be dominated by the bulk refraction effects of the denser large-scale fluctuations. Numerical calculations by Rusbridge (1968) have confirmed that the simple model of a randomly spaced assembly of discrete cylindrical plasma filaments provides a good representation of the microwave behaviour of a dense turbulent plasma. In terms of this model the plasma density may be written

$$n(\boldsymbol{r}) = \sum_{\alpha} \eta(\boldsymbol{r} - \boldsymbol{R}_\alpha)$$

where $\eta(\boldsymbol{r})$ is the density profile of a single plasma filament and $\boldsymbol{R}_\alpha$ ... etc. are a set of vectors randomly distributed with a number density N. The scattering cross section is given by Stott (1968)

$$\Gamma(\boldsymbol{k}-\boldsymbol{j}) = N\gamma(\boldsymbol{k}-\boldsymbol{j})$$

where $\gamma(\boldsymbol{k}-\boldsymbol{j})$ is the cross section of a single filament and $\boldsymbol{j}$, $\boldsymbol{k}$ are the initial and final wave vectors.

Heald (1964) has calculated the microwave refraction of large plasma cylinders for normal and oblique angles of incidence and has found that the mean scattering angle is almost independent of the exact shape of the density profile for cylinders with the same total density. Calculations by Faugeras (1965) show that the total cross section per unit length of the cylinder is approximately equal to the geometric diameter when the central density n_0 exceeds 10% of the critical density. Two lengths are therefore needed to characterize the model, the mean diameter of a cylinder d and the mean separation between cylinders s. These lengths are to be related in some way to the correlation distance of the density fluctuations a. To a first approximation the cylinders may be considered as touching each other and $d = s = a$.

The scattering cross section per unit volume of the plasma will therefore be taken as

$$\Gamma(\boldsymbol{k}-\boldsymbol{j}) = (d/\pi s^2)\gamma'(\boldsymbol{k}-\boldsymbol{j})$$

where $\gamma'(\boldsymbol{k}-\boldsymbol{j})$ is the scattering cross section of a plasma cylinder (normalized to $\int\gamma'(\boldsymbol{k}-\boldsymbol{j})\,\mathrm{d}\boldsymbol{j} = 1$) which is dependent on n_0/n_c and relatively independent of d and s.

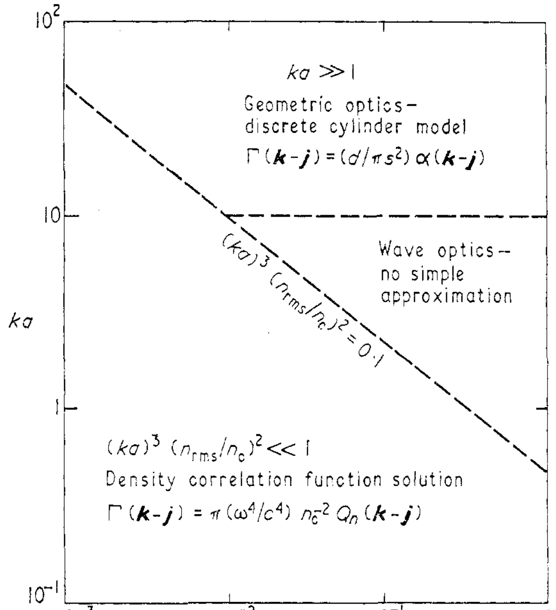

Figure 1. Criteria for the choice of approximation to the scattering cross section of turbulent plasma.

Figure 1 summarizes the approximations to the scattering cross section appropriate to the values of the parameters n_{rms}/n_c and ka. The turbulence parameters in ZETA and TPOT fit in the top right-hand corner of this figure.

3. Solution of the transport equation

The time-independent single-frequency transport equation for the photon distribution $f(\boldsymbol{r}, \boldsymbol{k})$, which is the probability density of finding a photon moving in the direction represented by the unit vector $\boldsymbol{k}$ at a point $\boldsymbol{r}$, has been given by Stott (1968):

$$\boldsymbol{k} \cdot \nabla f(\boldsymbol{r}, \boldsymbol{k}) + \int \gamma'(\boldsymbol{k}-\boldsymbol{j})\{f(\boldsymbol{r}, \boldsymbol{k}) - f(\boldsymbol{r}, \boldsymbol{j})\}\, \mathrm{d}\boldsymbol{j} = S(\boldsymbol{r}, \boldsymbol{k}). \tag{3.1}$$

The equation has been normalized by expressing the spatial dimensions in units of the mean free path between successive scatterings

$$\lambda = \{\gamma(\boldsymbol{k}-\boldsymbol{j})\, \mathrm{d}\boldsymbol{j}\}^{-1}$$
$$= \pi s^2/d.$$

$S(\boldsymbol{r}, \boldsymbol{k})$ is an external source or sink of photon flux.

The integral form of the transport equation is difficult to solve analytically except for a few rather simple cases which are poor approximations to the anisotropic scattering cross sections and boundary conditions occurring in experimental situations. The Monte Carlo type of numerical computation is particularly suitable for a solution of the transport equation under such conditions. The principles of the method are well known and certain special features associated with the present calculation are discussed in appendix 1. The Monte Carlo calculation is a mathematical analogue experiment, performed on a fast electronic computer, in which the individual trajectories of a large number of test particles, in this case photons, are followed through a random distribution of scattering centres, each of which is ascribed a cross section equal to $\Gamma(\boldsymbol{k}-\boldsymbol{j})$. It should be emphasized that these scattering centres are introduced only as a mathematical model of the multiple scattering process and are not in any way intended to represent a physical model of the turbulent plasma. In the present case, of course, there is a direct equivalence between these 'pseudo scatterers' and the elements of the model assumed for the turbulence, but the Monte Carlo solution would be equally valid for density fluctuations whose scattering cross section had been calculated in the full correlation function formalism.

When the receiving aerial is located at a large distance from the plasma, the scattering volume approximates to a point scatterer and the scattered microwave intensity depends only on the receiver position which will be denoted by the angles θ and θ', figure 4(*a*). Experimental considerations usually require the placing of the receiver as close to the plasma as possible and the received power then will depend on the orientation of the receiver denoted by the angles ϕ and ϕ' as well as its position, figure 4(*b*). These situations will be referred to as the far-zone and the near-zone respectively.

Figure 2 shows a typical far-zone distribution function calculated for parallel, straight cylindrical scatterers with a Gaussian cross section of characteristic width 10°. The source was repesented by a point source with an angular distribution of the form

$$S(\boldsymbol{r}, \boldsymbol{k}) = \delta(\boldsymbol{r})\delta(\alpha')\left(\frac{\sin \alpha/\alpha_{\mathrm{s}}}{\alpha/\alpha_{\mathrm{s}}}\right)^2$$

which with $\alpha_{\mathrm{s}} = 12°$ approximates the beam pattern of a typical microwave aerial at 2 mm wavelength.

For a plasma of small diameter D (i.e. a long photon mean free path), the distribution function can be split into two parts: a scattered component with a Gaussian profile and a directly transmitted beam attenuated by $\exp(-D)$. For larger diameter columns the attenuation is large and the distribution function achieves a Gaussian form independently of the precise shape of the scattering cross section. In figure 3 the Gaussian width θ_0 is plotted against the column diameter D, measured in mean free path units. The points, especially for large D, lie close to the line $\theta_0{}^2 = \psi_x{}^2 D$ which, with ψ_x equal to the mean deflection per single scattering, is a well known result given by diffusion theory in a plane-slab geometry.

The scattered microwave intensity received by an aerial in the near zone is obtained by integrating the distribution function over the beam pattern of the receiving aerial as in appendix 2. A typical plot of the near-zone scattered intensity in the plane $\theta' = \phi' = 0$ is shown in figure 5, the intensity being normalized with respect to the direct unscattered transmission between the aerials.

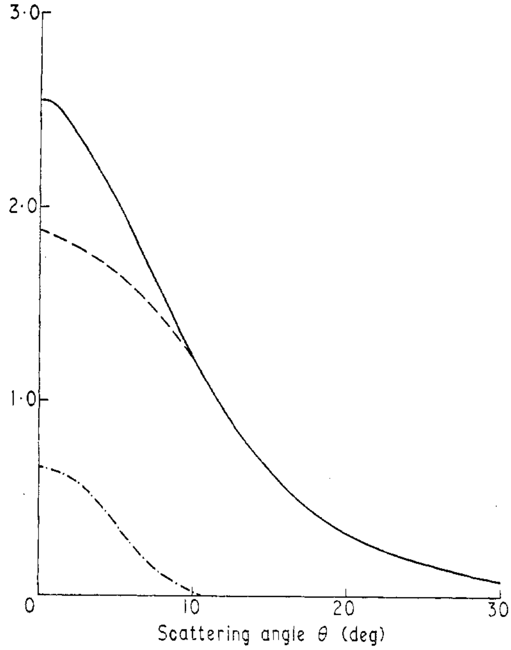

Figure 2. Far-zone distribution function for a plasma column of diameter $D = 2$ mean free paths, containing parallel straight cylindrical scatterers with mean scattering angle $\psi_x = 10°$. This can be split into two parts: – – – – scattered component with Gaussian profile width $\theta_0 = 14°$; –·–·–·– unscattered beam attenuated by $\exp(-2)$.

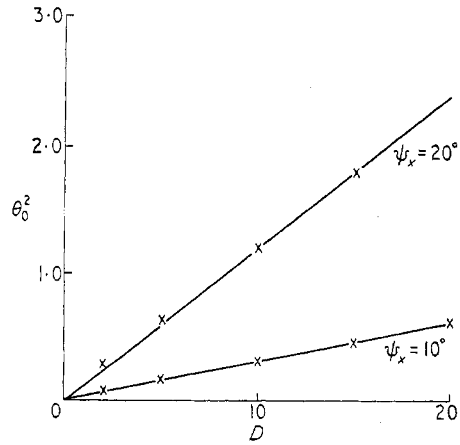

Figure 3. The variation of $\theta_0{}^2$ with D, predicted by diffusion theory. The crosses are the points calculated by the Monte Carlo method.

These results are all for zero pitch angle. Increasing the value of the helicity parameter Θ produces similar scattering along the axis of the plasma column.

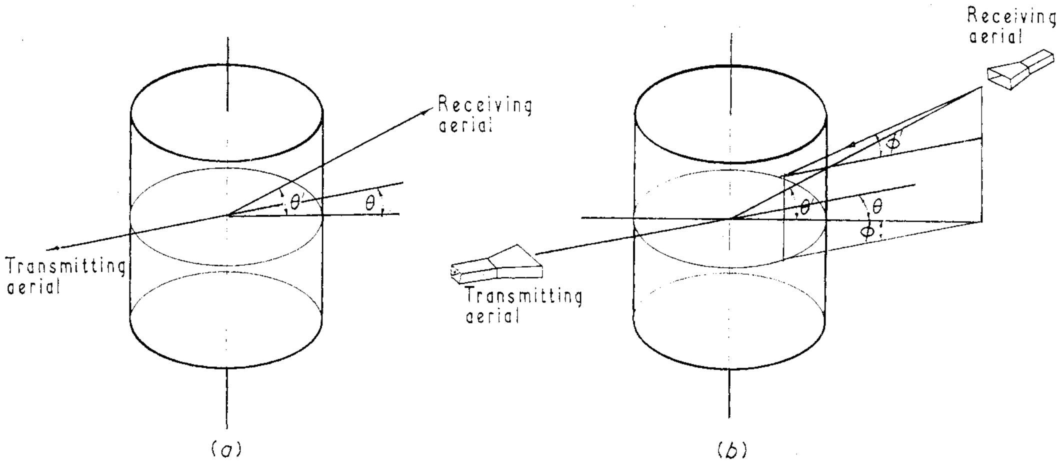

Figure 4. Scattering geometry for a cylindrical plasma column. (*a*) Near-zone scattering. (*b*) Far-zone scattering.

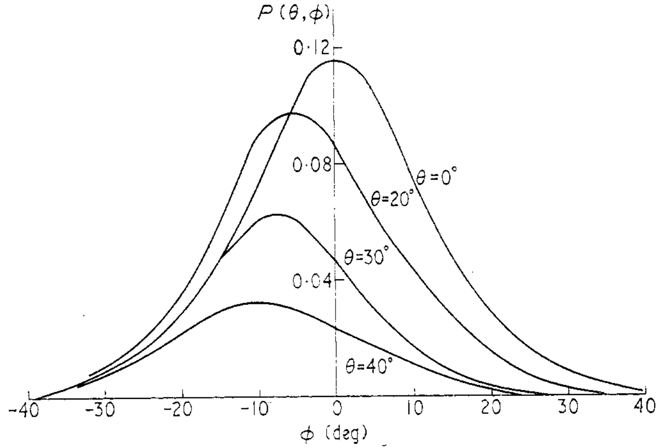

Figure 5. Near-zone scattered intensity $P(\theta, \phi)$ relative to direct transmission P_0. D = 10 mean free paths, ψ_z = 10°, calculated for transmitter and receiver aerials equivalent to WG16 waveguide at 2 mm wavelength.

4. Scattering experiments on ZETA

The details of ZETA have been described elsewhere (Butt *et al.* 1958), but briefly the device consists of a toroidal vacuum vessel (major and minor diameters of 3 and 1 metre respectively) filled with low-pressure deuterium gas in which high-current discharges can be induced, producing plasmas of density 10^{13}–10^{15} cm^{-3} at temperatures of 10–50 ev. The magnetic field due to the induced plasma currents is self-constricting and, helped by the conducting torus, is supposed to pull the plasma away from the walls. This configuration is hydromagnetically unstable, although partial stabilization is achieved by an externally applied axial field of 800 G. The helicity parameter Θ (= 1·7 in this case) characterizes the resultant magnetic configuration.

The transmitting aerial was mounted at the bottom of the torus, pointing vertically along a minor diameter, and the movable receiving aerial was located behind a quartz window in the same vertical plane (figure 6). Both aerials were open-ended sections of WG16 waveguide illuminated in the TE_{01} mode, which at 137 GHz (2·16 mm free-space wavelength) resulted in a beam width between first minima of 19° in the direction along the torus axis and 25° in the plane of the aerials. The transmitter was fed by a carcinotron backward wave oscillator (C.S.F. type COE 208) with a nominal rating of 5 watts output. Microwave losses in the waveguide and between the aerials reduced the signal level at the receiver to about 10^{-7} w. This was detected by a superheterodyne receiver, using a second carcinotron as local oscillator, followed by a balanced-crystal mixer and 408 MHz

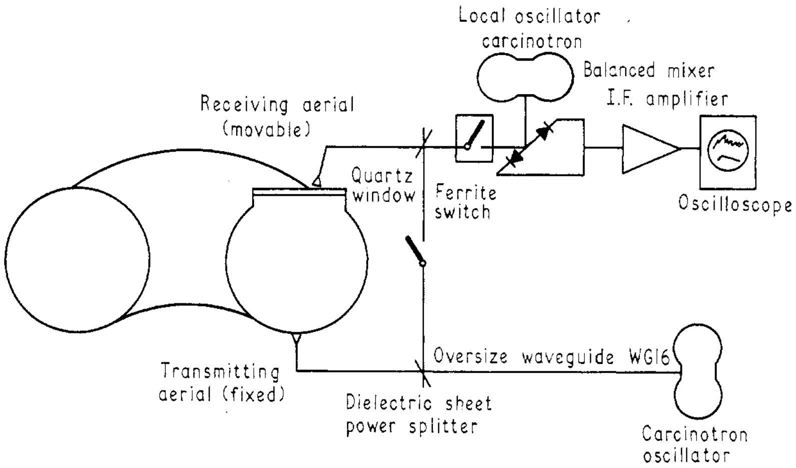

Figure 6. Millimetre wave scattering measurements on ZETA.

i.f. stage (Meredith *et al.* 1964). The relative stability of the two carcinotrons was monitored via a reference arm included in the waveguide circuit. During the period of strong transmission prior to the onset of turbulence, the sensitive receiver was protected by a ferrite microwave switch with an isolation of 27 dB which could be gated open for the duration of the ZETA current pulse.

The shot-to-shot reproducibility was found to be very good and statistical averages of the scattered signal were usually taken over three successive shots. The scattered profiles with the receiving aerial pointing at the centre of the discharge (i.e. $\phi = 0°$) were of Gaussian form

$$P(\theta, \phi = 0) = P(0)\exp(-\theta^2/\theta_0{}^2)$$

as verified in figure 7 by a logarithmic plot which gives $\theta_0 = 41°$ and $P(0) = 0{\cdot}15\%$ of the direct unscattered transmission. Values of θ_0 in the range 20°–60° and $P(0)$ of 0·05% to 0·20% were observed. A similar distribution along the direction of the torus axis was expected, but this region is inaccessible to microwave measurements on ZETA.

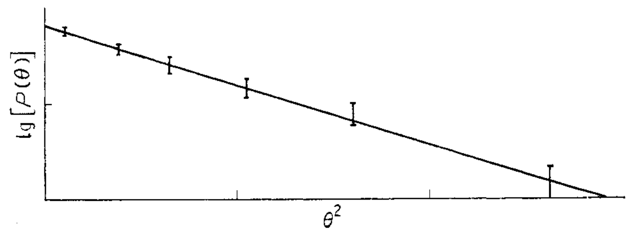

Figure 7. Typical logarithmic plot of scattered intensity on ZETA.

If the correlation length is taken as 5 cm and is assumed to remain approximately constant for a few milliseconds about the time of the peak plasma current, the scattering results can be interpreted, with the aid of the Monte Carlo calculations, in terms of r.m.s. values for the density fluctuations. The time-resolved plot in figure 8 reveals a period of reduced fluctuations occurring just after the peak plasma current which coincides with the quiescent period observed in ZETA (Wort 1965, Butt *et al.* 1965). In our case the quiescence appears to have been only partially established and this may be due to the pressure of impurities in the discharge.

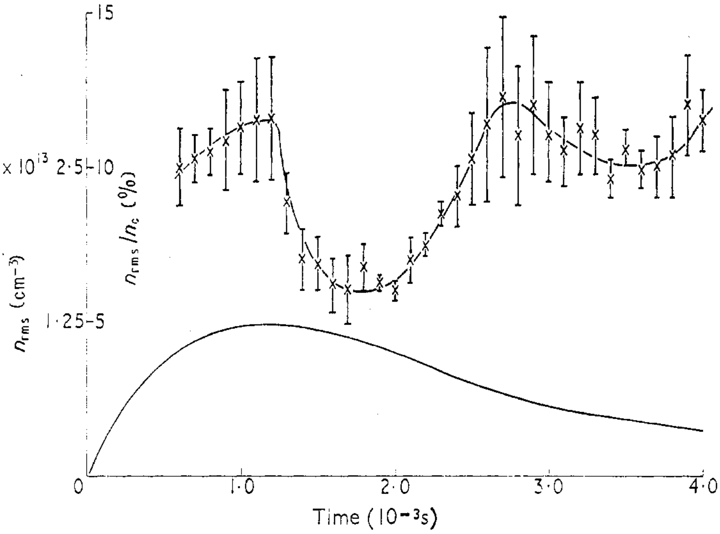

Figure 8. Time dependence of the r.m.s. density fluctuations in ZETA, calculated from the scattering measurements showing a quiescent period of reduced fluctuations. The lower trace is the plasma current, peak value 350 kA.

Wort (1965) has measured the density fluctuations in ZETA using a ray-optics small-angle approximation for the straight-through microwave transmission across the plasma, and his results, which are normalized with respect to the mean plasma density, are in very good agreement with the values obtained here.

5. Scattering experiments on TPOT

The TPOT device was constructed to provide a turbulent plasma readily accessible to microwaves. The vertically mounted Pyrex glass vacuum tube was 5 ft long and 1 ft in diameter. The centre section was of quartz so as to be transparent to millimetre waves. Discharge currents between the end electrodes of 10–15 kA produced hydrogen plasmas with densities in the range 10^{14}–10^{15} cm^{-3} at electron temperatures of around 3 ev. An axial magnetic field of up to 1 kG was provided by external coils.

The microwave aerials were mounted in a horizontal plane through the centre of the tube at a distance of 30 cm from the vertical axis. The fixed transmitting aerial had a beam width between first minima of 19° and 25° respectively in the horizontal and vertical directions. The receiving aerial, which had corresponding beam widths of 60° and 80°, could be rotated both about its own vertical axis and about the axis of the discharge tube, thereby covering all scattering angles. A VX 3352 point-contact germanium diode was used as a detector, the sensitivity at 137 GHz being improved to about 350 μV per μW by a forward bias current of 35 μA.

The statistics of scattering in the smaller diameter TPOT were less favourable than in ZETA, and as many as 100 separate shots were needed for accurate averaging. The large amount of data thus accumulated on oscilloscope films was translated to magnetic tape by an automatic flying spot film scanner and subsequently reduced to a manageable size by a digital computer.

Typical time-resolved plots in figure 9 of the scattering in the forward direction and at an angle $\theta = 20°$ show that a peak of scattering activity occurs about 400 μs after the start of the discharge with the scattering falling to zero over the next 300 μs. The signal received at the time of peak scattering activity with the aerial pointing radially to the plasma column is plotted in figure 10 against the scattering angle. The distribution splits into an exponentially attenuated transmission and a Gaussian scattered component, as predicted theoretically for a long photon-scattering free path. At scattering angles outside the main beam of the transmitting aerial (figure 11), there is a considerable increase in microwave intensity due to scattering.

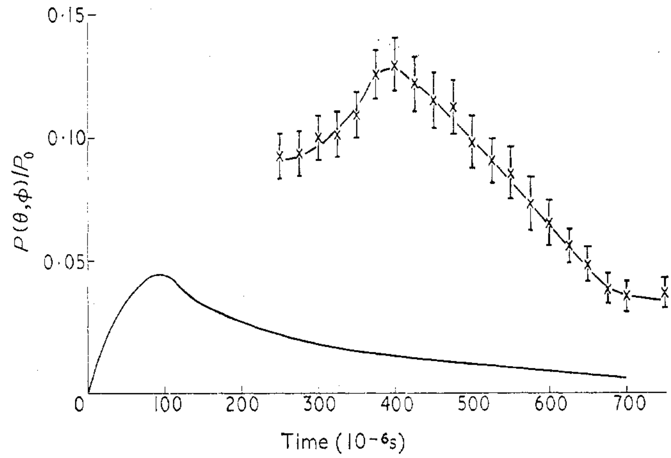

Figure 9. Time resolved scattering in TPOT, $\theta = 20°$, $\phi = 0°$. The lower trace is the plasma current, peak value 10 kA.

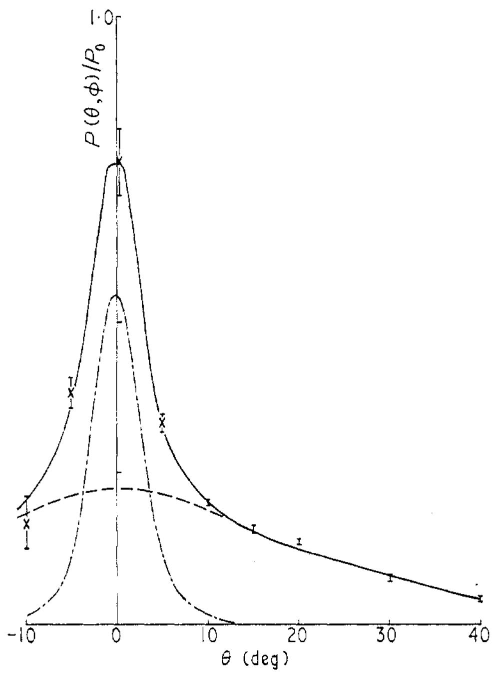

Figure 10. Scattered intensity in TPOT at $\phi = 0$ plotted against θ. Time = 400 μs. As theory predicts, this can be split into two parts: —·—·— attenuated direct transmission; – – – – scattered component with a Gaussian profile.

At the peak gas current of 10^4 A and with an axial magnetic field of some 500 G, the pitch angle of the helical magnetic field is about 15°, and the turbulence is very nearly two dimensional. It was confirmed experimentally that there was no microwave scattering outside the plane normal to the z axis of the discharge tube.

Interpreting these results in terms of the Monte Carlo solution indicates that the scattering was due mainly to a small number of discrete plasma filaments of diameter 5–10 cm and separated by 10–20 cm. At the time of 400 μs after the start of the discharge, the peak

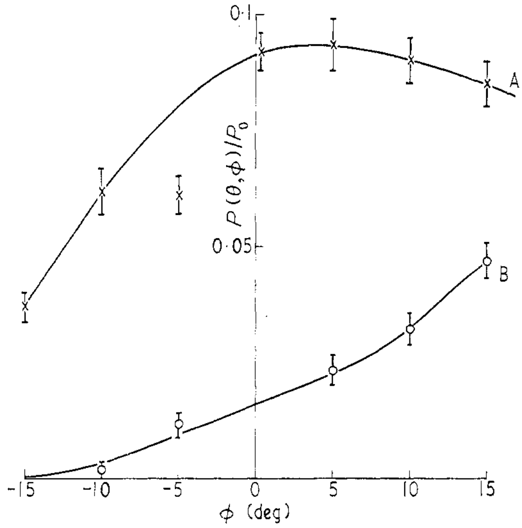

Figure 11. Scattered intensity in TPOT at $\theta = 20°$ plotted against ϕ. A, time $= 400\,\mu$s, i.e. during turbulent period. B, time $= 800\,\mu$s, i.e. during quiescent afterglow plasma.

plasma density calculated from the microwave measurements was $2{\cdot}0 \times 10^{14}$ which compares well with peaks of $2{\cdot}5 \times 10^{14}$ cm^{-3} about a mean density of $1{\cdot}0 \times 10^{14}$ cm^{-3} measured by a Langmuir probe. Both the probe and microwave results indicated that the density fluctuations decayed away smoothly over a time of 300 μs.

6. Conclusions

Microwave scattering techniques provide a useful method of investigating the density fluctuations of a turbulent plasma. The scattering can be interpreted successfully with the aid of the transport theory formulation of multiple scattering solved by a Monte Carlo method. Plasma effects such as collisional absorption of microwave energy and inelastic scattering could be included in the solution with very little modification, enabling calculation of the microwave emissivity and frequency broadening of a turbulent plasma.

The agreement between the microwave and Langmuir probe measurements confirms that the parallel cylinder model, although relatively crude, is a good representation of the microwave behaviour of a turbulent plasma in the limit of high-density long scale-length fluctuations.

Acknowledgments

The author would like to thank Professor S. F. Edwards, for his continued encouragement and interest in this work and also Mr. D. J. H. Wort for his invaluable advice and helpful criticism. The assistance and advice of Dr. E. S. Hotston and Mr. J. M. Weaver on microwave techniques is gratefully acknowledged.

Appendix 1. The Monte Carlo calculation

The mechanics of the Monte Carlo calculation are briefly as follows. A photon is released from the external source along a trajectory defined by the angles α and α' which are given by

$$\int_{-\pi}^{\alpha} S(\alpha)\,\mathrm{d}\alpha = p_i \int_{-\pi}^{+\pi} S(\alpha)\,\mathrm{d}\alpha$$

and

$$\int_{-\pi}^{\alpha'} S'(\alpha')\,\mathrm{d}\alpha' = p_i' \int_{-\pi}^{+\pi} S'(\alpha')\,\mathrm{d}\alpha'$$

where $S(\alpha, \alpha') = S(\alpha)S'(\alpha')$ is the beam pattern of the transmitting aerial (appendix 2). The set of numbers p_i, p_i' has a pseudo-random distribution in the interval $0 < p_i < 1$. On entering the plasma volume, the photon is allowed to travel a distance l between each scattering, where each value of l, in the mean free path units, is given by

$$\int_0^l \exp(-x)\,\mathrm{d}x = p_i \int_0^\infty \exp(-x)\,\mathrm{d}x.$$

At each scattering the deflection angle $\psi = \arccos(\boldsymbol{k}.\boldsymbol{j})$ is calculated from the normalized scattering cross section $\gamma'(\boldsymbol{k},\boldsymbol{j})$

$$\int_{-\pi}^{\psi} \gamma'(\psi')\,\mathrm{d}\psi' = p_i$$

and the new trajectory computed.

The probability of a photon escaping from the plasma can be varied to simulate transparent or partially reflecting walls. When the photon leaves the plasma volume, the coordinates and direction angles specifying the exit trajectory are calculated and, after following a large number of photons (typically 5–10 000) these are sorted into a series of histograms which give the photon distribution function. Integration of the distribution function over the acceptance angles of the receiver gives the scattered intensity.

Frequency dispersion due to temporial density fluctuations can easily be accommodated and the introduction of a small photon absorption cross section permits calculation of the microwave emissivity of turbulent plasma.

Appendix 2. Microwave aerials

Microwave beams at millimetre wavelengths are commonly launched and received by open-ended apertures of rectangular section waveguide. At distances greater than the Rayleigh distance ($2\Delta^2/\lambda$ where Δ is the larger dimension of the aperture and λ is the free-space wavelength) the aerial may be represented as a point source with a beam limited in width by the diffraction pattern of the aperture, which for uniform illumination is

$$S(\alpha, \alpha') = \left\{\frac{\sin(\pi\Delta\lambda^{-1}\sin\alpha)}{\pi\Delta\lambda^{-1}\sin\alpha}\right\}^2 \left\{\frac{\sin(\pi\Delta'\lambda^{-1}\sin\alpha')}{\pi\Delta'\lambda^{-1}\sin\alpha'}\right\}^2 \tag{A1}$$

where Δ and Δ' are the dimensions of the aperture. The direction of observation $\boldsymbol{k}$ is defined relative to the forward direction $\boldsymbol{k}_0$ by the angles α and α' in planes parallel to the edges of the aperture. In the TE_{01} mode, the electric field parallel to the shorter dimension has a cosine distribution along the longer dimension, which approximately reduces the effect width by a factor of about 0·6.

The gain of an aerial in direction $\boldsymbol{k}$ will be written as

$$G(\boldsymbol{k}) = G(0)S(\boldsymbol{k})$$

where $G(0)$ is the gain in the forward direction $\alpha = \alpha' = 0$. The effective collecting area of a receiver is

$$A_{\mathrm{R}} = (4\pi)^{-1}\lambda^2 G(\boldsymbol{k}).$$

The power received by an aerial of area A_{R} at $\boldsymbol{R}_{\mathrm{R}}$ pointing in a direction $\boldsymbol{k}_{\mathrm{R}}$ will be

$$P(\boldsymbol{R}_{\mathrm{R}}, \boldsymbol{k}_{\mathrm{R}}) = G_{\mathrm{R}} \left(\frac{\lambda}{4\pi \boldsymbol{R}_{\mathrm{R}}}\right)^2 \int_{4\pi} f(\boldsymbol{R}_{\mathrm{R}}, \boldsymbol{l}) S_{\mathrm{R}}(\boldsymbol{l} - \boldsymbol{k}_{\mathrm{R}})\,\mathrm{d}\boldsymbol{l}.$$

It is convenient to normalize the scattered power relative to the direct transmission P_0 between the two aerials (denoted by subscripts T and R respectively) pointing towards each other in free space.

$$P(\boldsymbol{R}_R, \boldsymbol{k}_R) = P_0(G_T)^{-1}\left(\frac{R_R+R_T}{R_R}\right)^2 \int_{4\pi} f(\boldsymbol{R}_R, \boldsymbol{l})S_R(\boldsymbol{l}-\boldsymbol{k}_R)\, d\boldsymbol{l}. \tag{A2}$$

In the far zone ($R_R \gg R_T$), $f(\boldsymbol{r}, \boldsymbol{k})$ becomes effectively a δ-function of $\boldsymbol{k}$, $\boldsymbol{k} = \boldsymbol{r}/|r|$ and the scattered power is

$$P(\boldsymbol{R}) = P_0(G_T)^{-1}f(\boldsymbol{R}). \tag{A3}$$

For two-dimensional scattering the corresponding expression to (A2) is

$$P(R_R, \phi) = P_0\left(\frac{R_T+R_R}{R_R}\right)(G_T)^{-1}\int_0^{2\pi} f(R_R, \alpha)S_R(\alpha, -\phi)\, d\alpha \tag{A4}$$

References

BUTT, E. P., *et al.*, 1958, *2nd Int. Conf. on the Peaceful Uses of Atomic Energy, Geneva*, **32,** 42–64 (Geneva: United Nations).

BUTT, E. P., *et al.*, 1965, *Proc. Int. Conf. on Plasma Physics, Culham*, 1965, Vol. 2 (Vienna: International Atomic Energy Agency), pp. 751–64.

FAUGERAS, P. E., 1965, *Proc. 7th Int. Conf. on Phenomena in Ionized Gases, Belgrade*, **3,** 113 (Belgrade: Gradevinska Knjiga) see also CEA *Rep.* No. EUR-CEA-FC-351.

HEALD, M. A., 1964, *Culham Lab. Rep.* CLM-R34.

LARIONOV, M. M., *et al.*, 1968, *Sov. Phys.–JETP*, **12,** 1067–71.

MEREDITH, R., *et al.*, 1964, *Proc. Inst. Elect. Eng.* **3,** 241–56.

ROBINSON, D. C., and RUSBRIDGE, M. G., 1965, *Proc. 7th Int. Conf. on Phenomena in Ionized Gases, Belgrade*, **2,** 204 (Belgrade: Gradevinska Knjiga).

RUSBRIDGE, M. G., 1968, *Plasma Phys.*, **10,** 95–108.

STOTT, P. E., 1968, *J. Phys.* A (*Proc. Phys. Soc.*), [2], **1,** 675–89.

WORT, D. J. H., 1965, *Proc. 7th Int. Conf. on Phenomena in Ionized Gases, Belgrade*, **3,** 130 (Belgrade: Gradevinska Knjiga).

—— 1966, *Plasma Phys.*, **8,** 79–93.